

## INFLUENCES OF THE GAIN COEFFICIENT ON THE NONLINEAR OSCILLATOR'S DYNAMICAL REGIMES OF MACH-ZEHNDER MODULATOR MZM WITH OPTOELECTRONIC FEEDBACK

**Layla Omar BABARASUL**<sup>1</sup>

University of Garmiyah, Iraq

**Younis Thanoon YOUNIS**<sup>2</sup>

University of Mosul, Iraq

### Abstract:

In this research we have modeled the Mach-Zehnder Modulator MZM with optoelectronic feedback OEF as optoelectronic oscillator OEO. The model is based on the Integro-Differential equation, which includes nonlinear effects from MZM device with time delay feedback arise from optoelectronic feedback OEF. Numerical simulation of our OEO model demonstrated wide regimes of complex oscillations, ranged from period one, period doubling, mixed mode, quasi-period and chaotic oscillations, that is with increasing the value of the linear gain coefficient. This effect was verified by the bifurcation diagram of maxima values of RF-voltages versus control parameter which in this case is the linear gain coefficient value, which depicted the route to chaos of OEO system.

**Keywords:** Optoelectronic Feedback, Optoelectronic Oscillator, Chaos Control.

---

 <http://dx.doi.org/10.47832/2717-8234.13.17>

<sup>1</sup>  [layla.20esp30@student.uomosul.edu.iq](mailto:layla.20esp30@student.uomosul.edu.iq)

<sup>2</sup>  [younisthannon@uomosul.edu.iq](mailto:younisthannon@uomosul.edu.iq), <https://orcid.org/0000-0002-4790-4475>

**1- Introduction:**

In the last few decades, utilizing Mach-Zehnder modulator have been increased as unique optoelectronic device in multidisciplinary fields e.g. integrated optics IO, microwave signal generation [1-3], all optical signal processing, high data rate optical telecommunication [4, 5]. Reservoir computing hardware based Artificial Neural Network (ANN) recruiting optical chaotic systems have been reported [6, 7]. Nonlinear systems with time delayed feedback exhibits diversity dynamical phenomena [11]. Ikeda model is an earliest paradigm of the nonlinear system with delayed feedback, which describes laser instabilities under ring cavity optical feedback [12]. One of the most efficient tools for generating optical chaotic signals is the optoelectronic oscillator OEO, based on delay time nonlinearities, through returning portion of electrical signal (that detected from optical output after delayed time by optical fiber which acts as delay line of the system) and fed it back into modulation input term of the electro-optical modulator, such kind of systems exhibits various kinds of instabilities, such as bistability, periodic oscillation, quasi-periodic, and high dimensional chaotic oscillations [8]. In accordance to Ikeda-like model, there are four requirements to construct OEO, which are nonlinear functional  $f_{NL}$  medium, delay line  $\tau_D$ , linear gain amplification  $\beta$  and linear filter response  $\{\hat{M}\{x(t)\}$ , have to be available for building up optoelectronic oscillation system, this can be seen in Figure (1) Such that they satisfy the interrelated as [1]:

$$\hat{M}\{x(t)\} = \beta f_{NL}(x(t - \tau_D)) \tag{1}$$

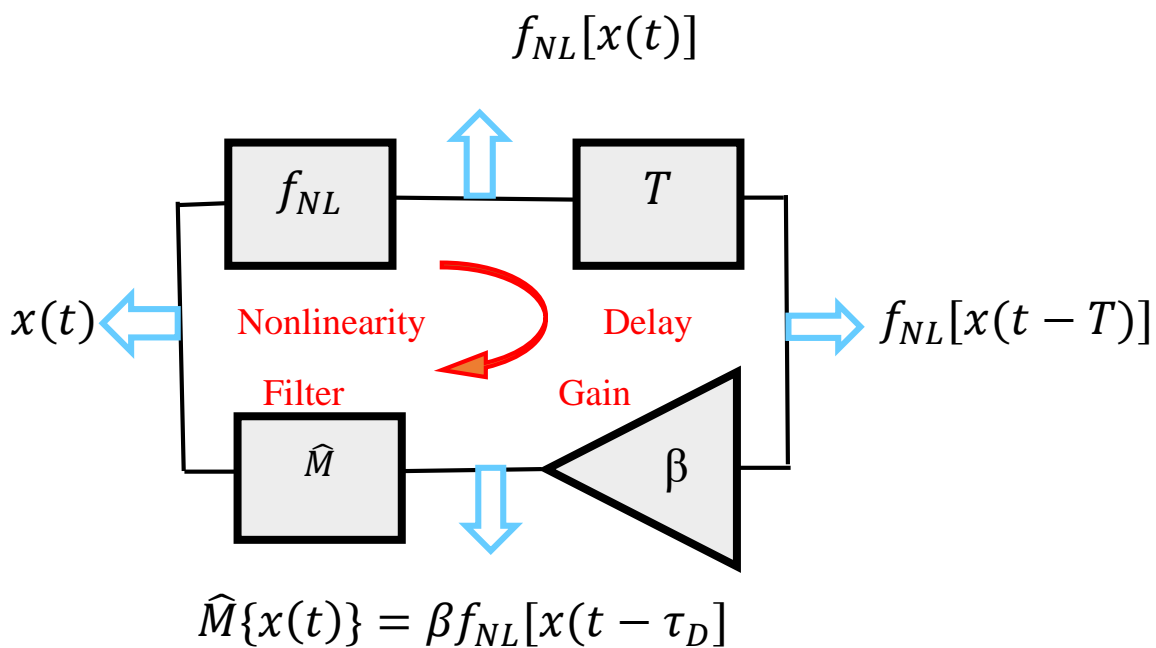


**Fig. (1): block diagram of OEO based Ikeda-like model [1].**

**2- Model and setup:**

In this research work, we have modeled MZM with a close loop optoelectronic feedback (OEFB) circuit diagram as OEO system which constructed as shown in Figure (2) from symmetric MZM modulator connected to single mode fiber optic (SMF) of 4km length insures 20µs delay time, the other terminal of the fiber connected with fast response photodetector (PD) which intern connected to band pass filter (BPF) that support about <0.6 MHz band width of radio frequency (RF) resolution. The output signal from BPF amplified by RF amplifier with

gain (G), the amplified signal V(t) which in turn has frequencies in microwave band, this signal fed into RF-input electrode of MZM device. The transmission behavior of MZM is a nonlinear function with applied voltage V(t), and the transfer function of the OEO is given by the integro-differential Eq.(1) [11]:

$$x(t) + \tau_H \frac{d}{dt} x(t) + \frac{1}{\tau_L} \int_{t_0}^t x(s) ds = \beta \cos^2 [ x(t - \tau_D) + \phi ] \quad (2)$$

where  $x(t) = \frac{\pi v(t)}{2 v_{\pi RF}}$  and  $\phi = \frac{\pi v_{DC}}{2 v_{\pi DC}}$  are dimensionless dynamical variable for and phase constant of the system signal respectively.  $\beta = \frac{\pi \eta \gamma G S P_i}{2 v_{\pi RF}}$  is the linear gain coefficient, with  $\eta$  which is MZM transmission coefficient,  $\gamma$  is optical fiber transmission coefficient, S is the photodetector sensitivity and  $P_i$  is the input power of laser diode LD.

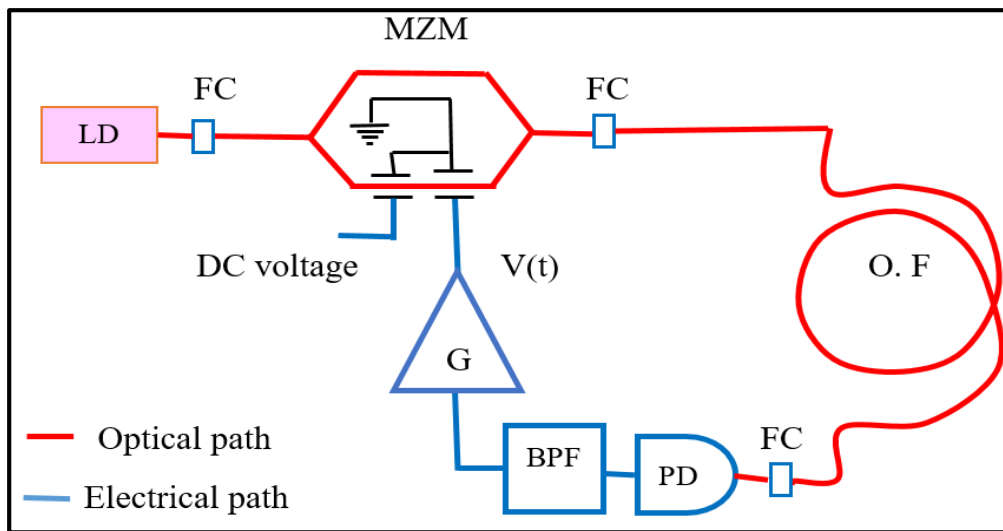


**Fig. (2): OEO architecture diagram LD is laser diode, MZM is the Mach-Zehnder modulator, FC is fiber connector, PD is the photodetector, BPF is band pass filter, and G is the gain of RF amplifier.**

and its half-wave DC and RF voltages are  $V_{\pi DC}$  and  $v_{\pi RF}$  respectively

$\tau_H = \frac{1}{2\pi f_H}$  and  $\tau_L = \frac{1}{2\pi f_L}$  are response time constants for high  $f_H$  and low  $f_L$  cutoff frequencies respectively.  $\tau_D$  is delay time arising from optical fiber of length L. introducing new time variable  $t'$  in units of time delay  $\tau_D$ , i.e.  $t' = t/\tau_D$ , equation (2) can be rewritten as:

$$x(t') + \varepsilon \frac{d}{dt} x(t') + \delta \int_{t_0}^{t'} x(s') ds' = \beta \cos^2 [ x(t' - 1) + \phi ] \quad (3)$$

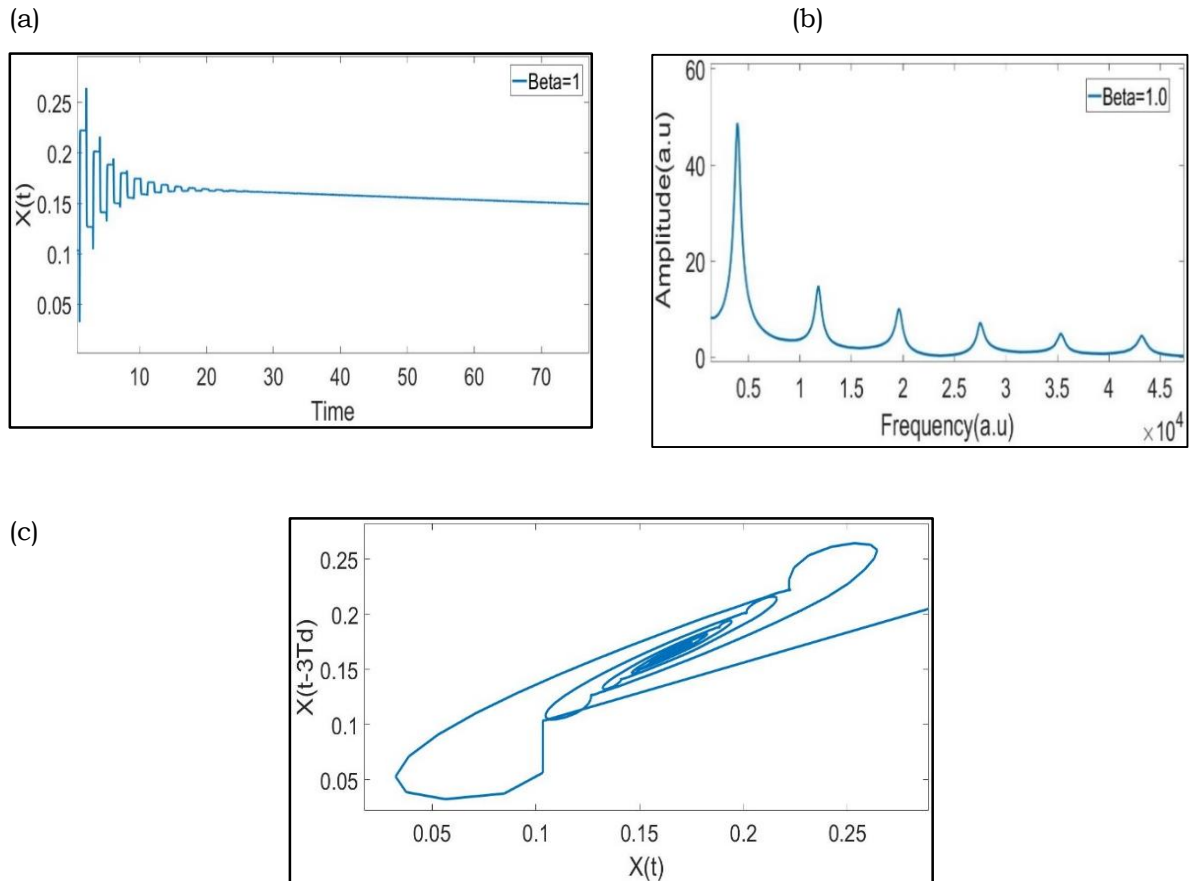
Where  $\varepsilon = \frac{\tau_H}{\tau_D}$  and  $\delta = \frac{\tau_D}{\tau_L}$  are new dimensionless parameters. The last equation is dimensionless nonlinear delayed integro-differential equation which describes slow-fast oscillation dynamics. The last equation Eq. (3) can be solved numerically by delayed differential equation DDE solver package in MATLAB program. For the numerical solution purposes, Table (1) involves the main parameters values utilized in the modeling and numerical simulation of the system (3).

Table 1 The values of the main parameters of simulation model (3)

Parameter	Value
<b>Laser Diode input power</b>	<b>5mW</b>
<b>MZM transmission coefficient <math>\eta</math></b>	
<b>MZM splitting ratio (equal)</b>	<b>50%</b>
<b>MZM DC half wave voltage <math>V_{\pi DC}</math></b>	
<b>MZM RF half wave voltage <math>V_{\pi RF}</math></b>	
<b>Optical fibre losses coefficient <math>\gamma</math></b>	
<b>Optical fibre length L</b>	<b>4.0Km</b>
<b>Delay line time <math>\tau_D</math></b>	<b>20.0<math>\mu</math>s</b>
<b>Photodetector sensitivity S</b>	<b>1.05</b> <b>Volt/mW</b>
<b>Low pass filter LPF cut-off frequency <math>f_L</math></b>	<b>22Hz</b>
<b>High pass filter HPF cutoff frequency <math>f_H</math></b>	<b>0.6MHz</b>
<b>RF amplifier gain G</b>	<b>3.0</b>

### 3- Results and discussion

To study the effect of the linear gain coefficient  $\beta$  on the behavior of a nonlinear system through numerical simulation of the DDE solver program of Eq(3), all variables been setting fixed as in Table (1), while the value of linear gain  $\beta$  changed each time of DDE solver running. Setting linear gain coefficient  $\beta$  to 1 and executing our MATLAB code DDE solver to solve system of Eq.(3), we get the **Figure (3a)** that shows time series of the generated damped RF signal  $x(\xi)$  which appears as spiky edged square oscillations, the damping occurs due to the waning in value of  $\beta$  which depends mainly on the values of the amplifier gain G and laser input power  $P_i$ . Figure (3b) shows the fast Fourier transform FFT or spectrum of the signal  $x(\xi)$ , this figure appears main oscillation peak at frequency of 4000, besides other small amplitudes of its harmonics. While Figure (3c) shows the attractor diagram as inner spiral loop of damped oscillation indicating to case of stable point dynamic [13].



**Fig.(3) Generated signal by OEO system at the value of nonlinear coefficient  $\beta=1$  (a) time series  $X(t)$ , (b) FFT frequency spectrum of the signal  $X(t)$ , (c) Attractor trajectory of the signal  $X(t)$ .**

Increasing the value of nonlinear coefficient  $\beta$  to 1.6 and executing the simulation, we get time series of periodic continuous oscillation as seen in **Figure (4a)**, and its FFT spectrum as in **Figure (4b)** where the main frequency about 3900 with maxima heights amplitude and its harmonics with low amplitudes. **Figure (4c)** shows thick traced limit cycle trajectory attractor.

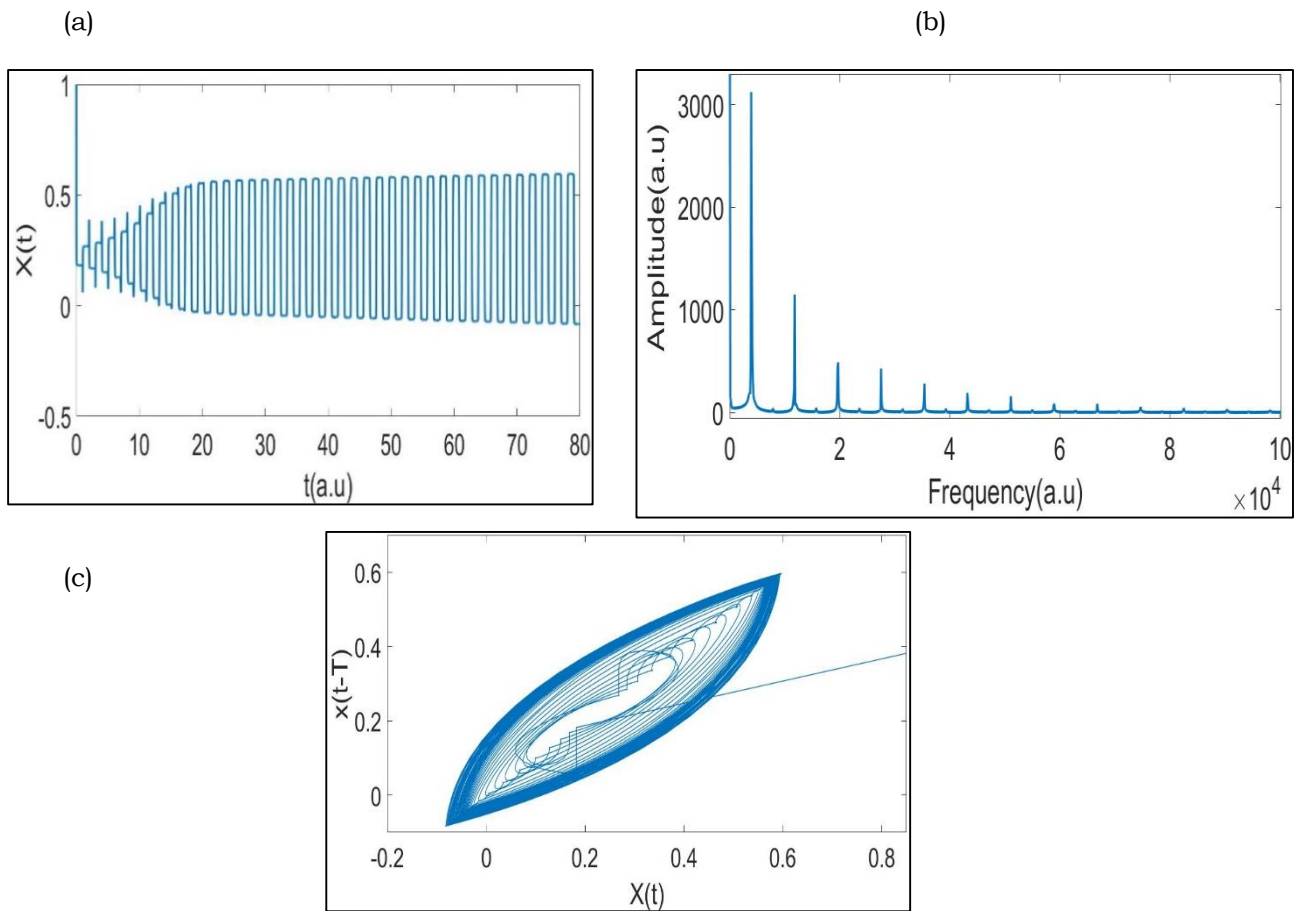


**Fig. (4) generated signal from OEO  $X(t)$  at  $\beta=1.6$  (a) time series of periodic oscillation signal  $X(t)$ , (b) FFT spectrum of  $X(t)$ , (c) limit cycle trajectory attractor.**

More increasing of  $\beta$  to 2.2 and executing numerical solver we get the Figure (3a) (4a) which shows period two oscillation dynamic of generated signal  $X(t)$  as two different amplitudes oscillation, and Figure (3b) shows FFT spectrum of the generated signal  $X(t)$ , and Figure (3c) (4c) الشكل appears attractor of two main thick entangled limit cycles, while the middle centered loops represent initial oscillation peaks.

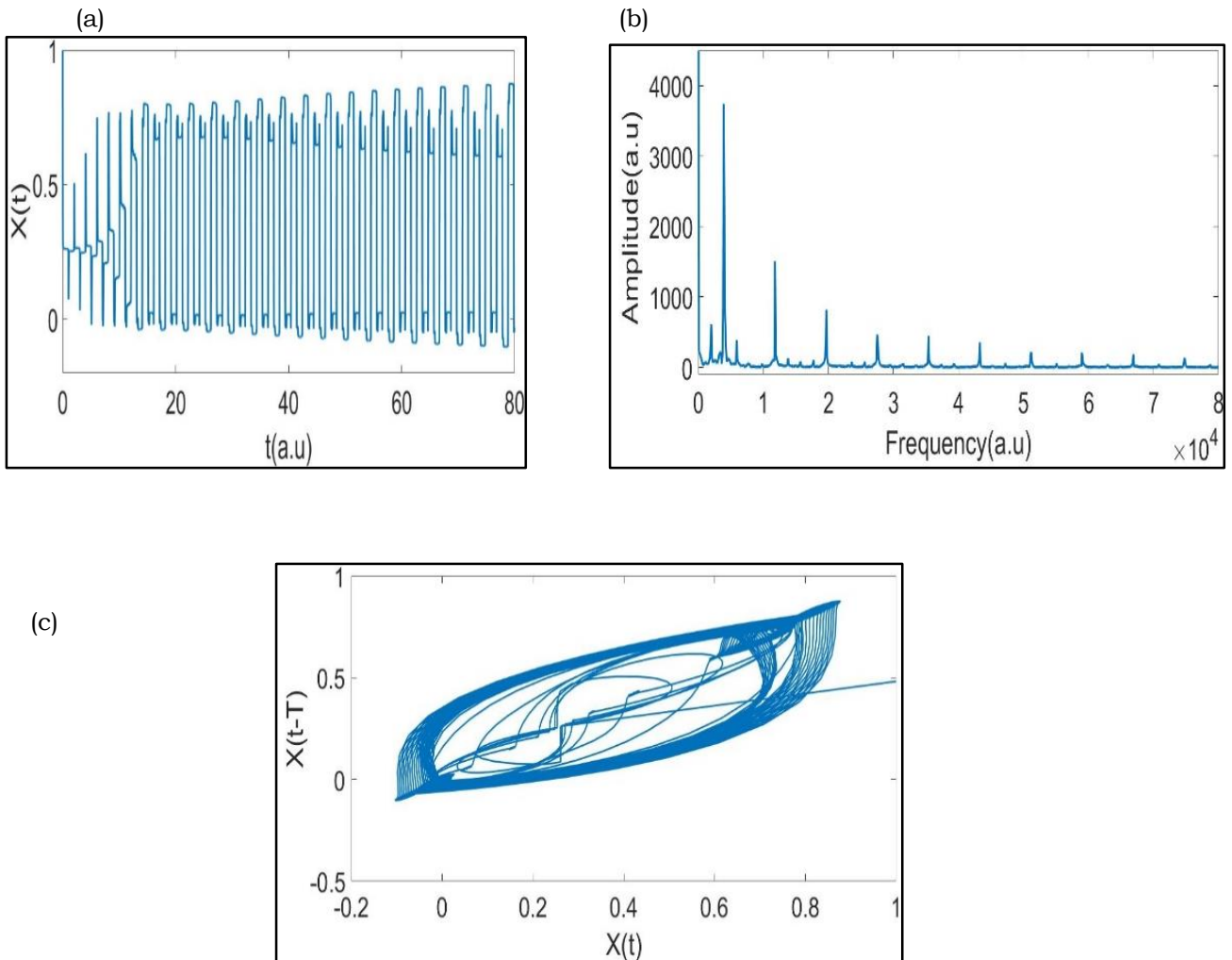


**Figure (5): generated signal of OEO  $X(t)$  at  $\beta=2.2$  (a) time series period two  $X(t)$  as two different amplitudes and (b) is its FFT spectrum, (c) phase attractor as two crossed limit cycles.**

By more increasing of nonlinear coefficient  $\beta$  to 2.4 and running the numerical DDE solver we get the **Figure (4a)** which exhibits period two oscillation conjugated with appearing superimposed fast oscillation picked-up on the periodic amplitudes, **Figure (4b)** shows FFT spectrum of the generated signal  $X(t)$  as periodic oscillation frequency components as well as small amplitudes of new frequency components of fast oscillations. **Figure (3-4c)** shows the trajectories of the two main entangled limit cycles as long loops with the short closed loops of the fast oscillation, such kind of oscillation is called slow-fast or mixed mode oscillation (MMO) [13].

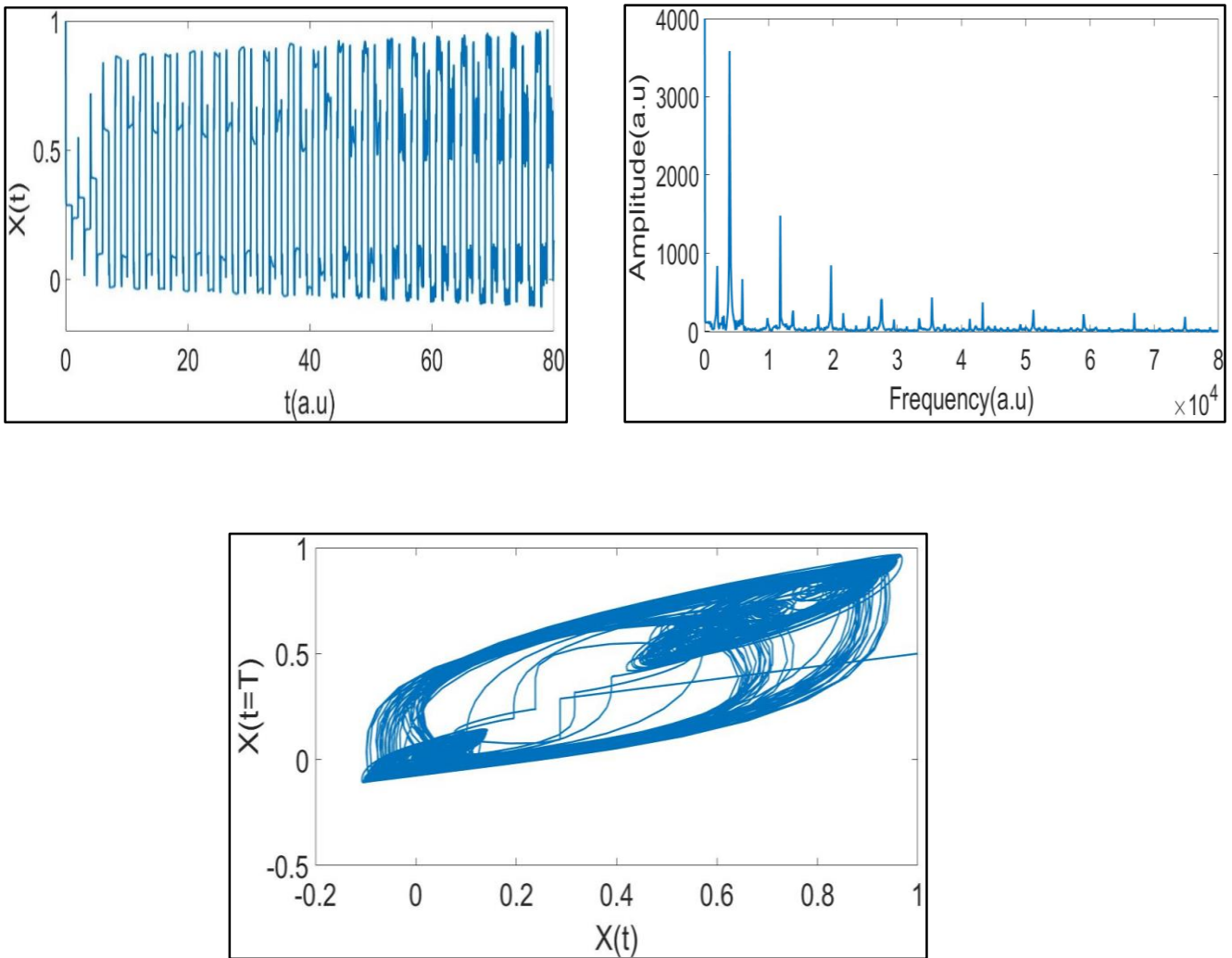


**Figure (6):** OEO generated signal at  $\beta=2.4$  (a) time series of Mixed Mode oscillation MMO signal  $X(t)$  (b) FFT spectrum of  $X(t)$  (c) Attractor portraits of  $X(t)$ .

By putting the nonlinear coefficient  $\beta=2.6$  and executing our DDE solver we get the **Figure (7a)** which explains time evolution of inception of transition to produced semi-periodic oscillations  $X(t)$  as high randomness fast fluctuations picked up on periodic signals, and its FFT spectrum is shown in **Figure (7b)** where the frequency components of the generated signal are presented.



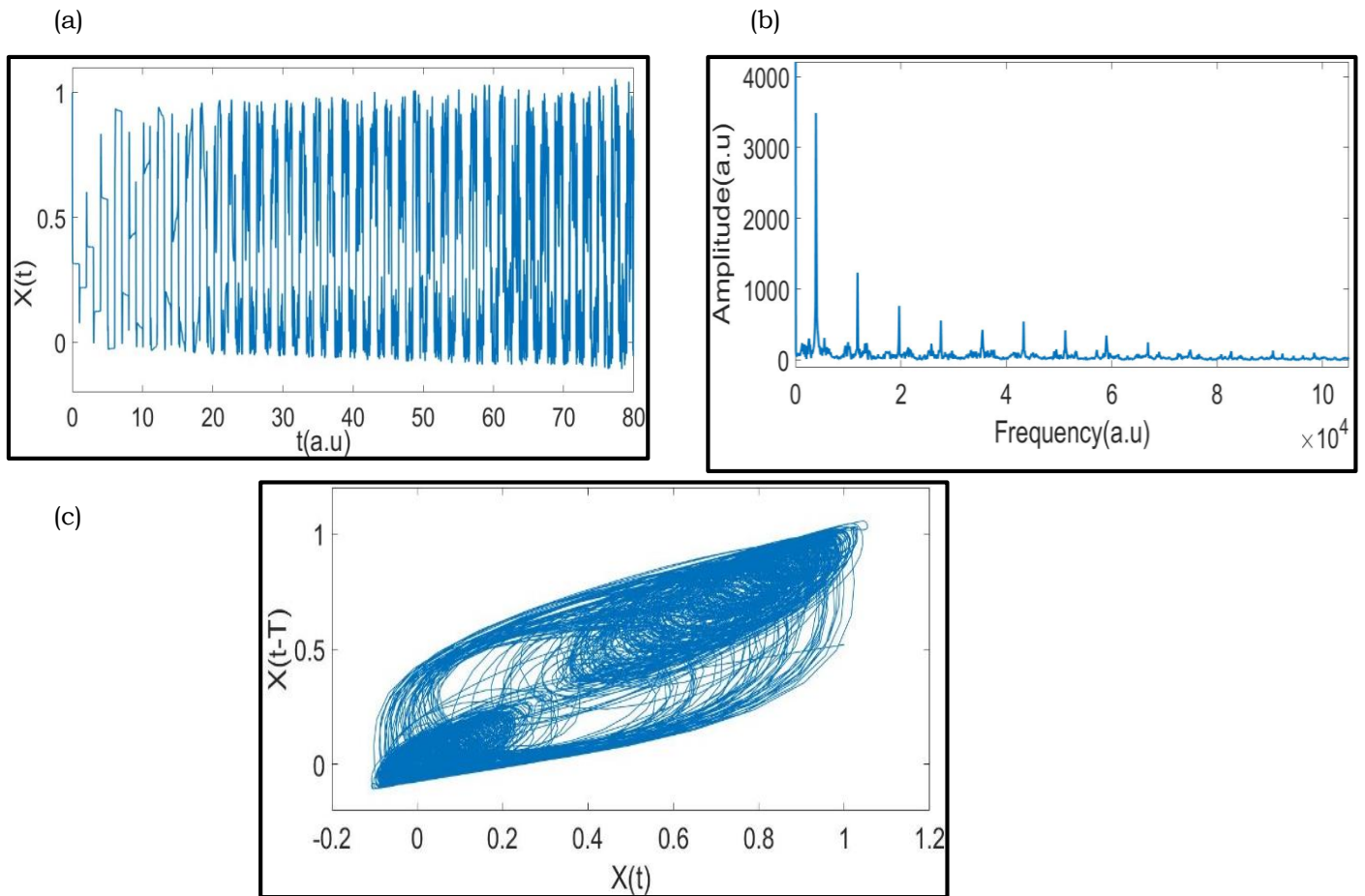


**Fig. (7): OEO generated signal at  $\beta=2.6$  (a) time series of quasi-periodic oscillation of the signal  $X(t)$  (b) FFT spectrum of  $X(t)$ , (c) Attractor trajectories of  $X(t)$  plotted by embedded technique.**

Putting the value of nonlinear coefficient  $\beta$  equal to 2.8 and running the DDE solver we get Figure (8a) which exhibiting chaotic oscillation time evolution  $X(t)$  where this oscillation is full randomness, this is very clear by the FFT spectrum in Figure (8b) where many new fast oscillation frequencies with high amplitudes started to appear as fingerprint of chaotic oscillation. Figure (8c) shows dense overlapped trajectories attractor which reveals chaotic oscillation occurrence.

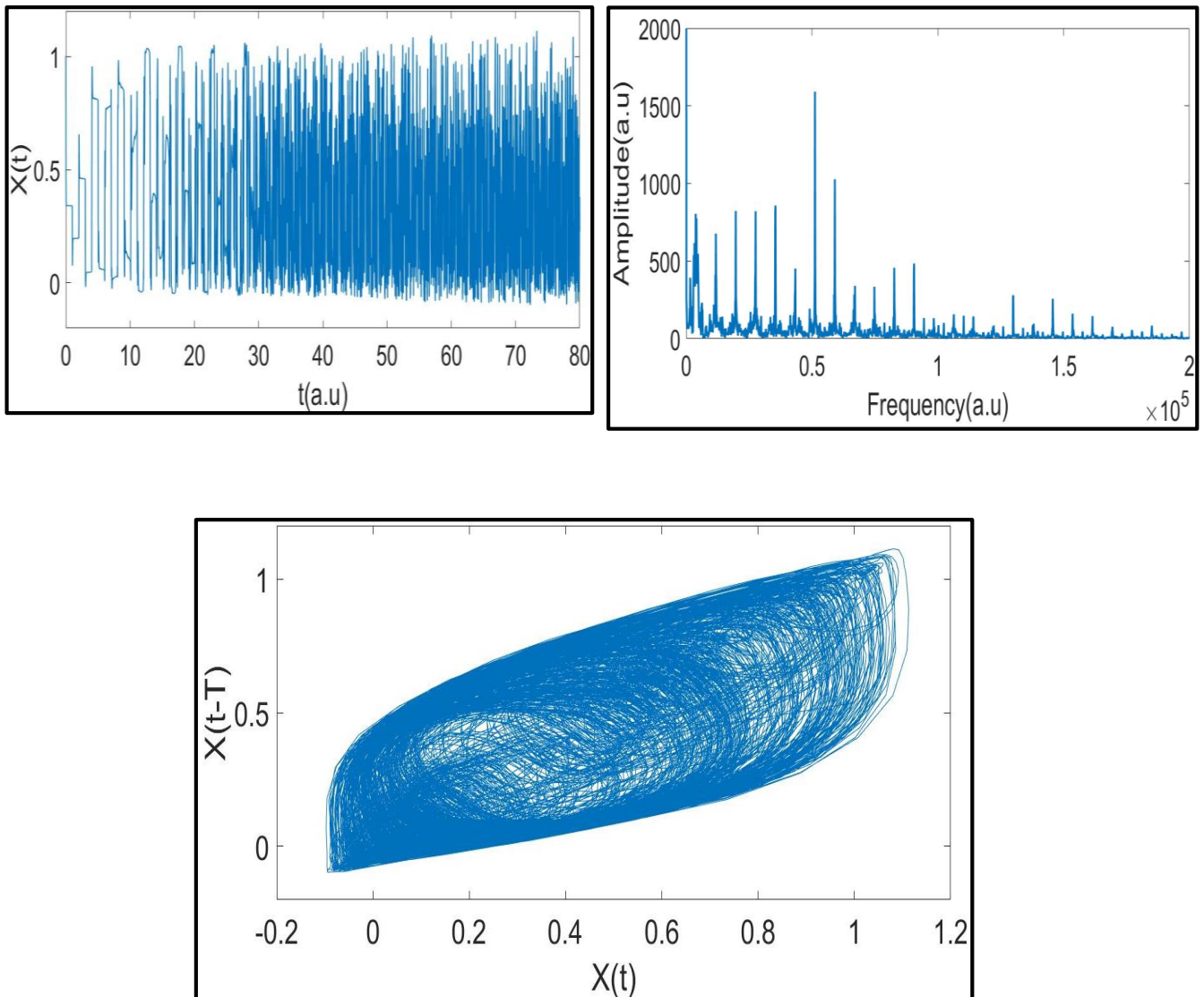


**Figure (8) OEO generated signal  $X(t)$  at  $\beta=2.8$  (a) time series of chaotic oscillation of the signal  $X(t)$ , (b) FFT spectrum of  $X(t)$ , (c) dense overlapped trajectories of chaotic signal  $X(t)$ .**

The overall dynamical behavior of our OEO system have been demonstrated by the sketching the bifurcation diagram as depicted in the Figure (9) which exhibiting distribution of maxima values of generated signals  $\max(X(t))$  as a function of control parameter which is in this case is the nonlinear coefficient  $\beta$ . As it can be seen in the Figure (9) when the control parameter  $\beta$  value ranges from 1.0 to 1.28, the system being in the periodic oscillation state. Beyond this value and reaching to  $\beta$  value of 2.12, the dynamical state of the system converted to period two or period doubling oscillation which is known as Pitchfork bifurcation [14].

For the case of control parameter  $\beta$  ranges from 2.12 to 2.26 the thickness of the bifurcation traces seen to be increased due to appearing fast oscillation conjugated with period two oscillation. For the values of  $\beta$  ranges from 2.26 to 2.36 the system jumps to multi-periodic oscillation as a result of increasing the amplitudes of fast oscillation against slow-oscillation amplitudes, therefore many different oscillating amplitudes will be appearing as a thickness in trace of  $\text{Max}(X(t))$ -axis in Figure (9). For the case of  $\beta$  values ranged from 2.36 to

2.66, as can be seen from the bifurcation Figure (9) the number of bifurcating points (oscillation magnitudes) seems to be increased monotonically, indicating to quasi-periodic oscillation state occurrence of the system, this is so, because of accretion of the randomness fast oscillation amplitudes. For the values of  $\beta$  beyond 2.66 reaching to 3.5 the number of bifurcating points being significantly increased and the dynamical system state of OEO exhibits chaotic oscillation, as a result of randomness fast-oscillation amplitudes crises with slow oscillation amplitudes. The sudden transition of our OEO system from chaotic oscillation to hyper-chaotic oscillation occurred after slight increment of the  $\beta$  beyond 3.5, causing increasing huge the numbers of bifurcating fast-oscillation amplitudes ( $\text{Max}(X(t))$ ) of the OEO system, as can explained in Figure (9).

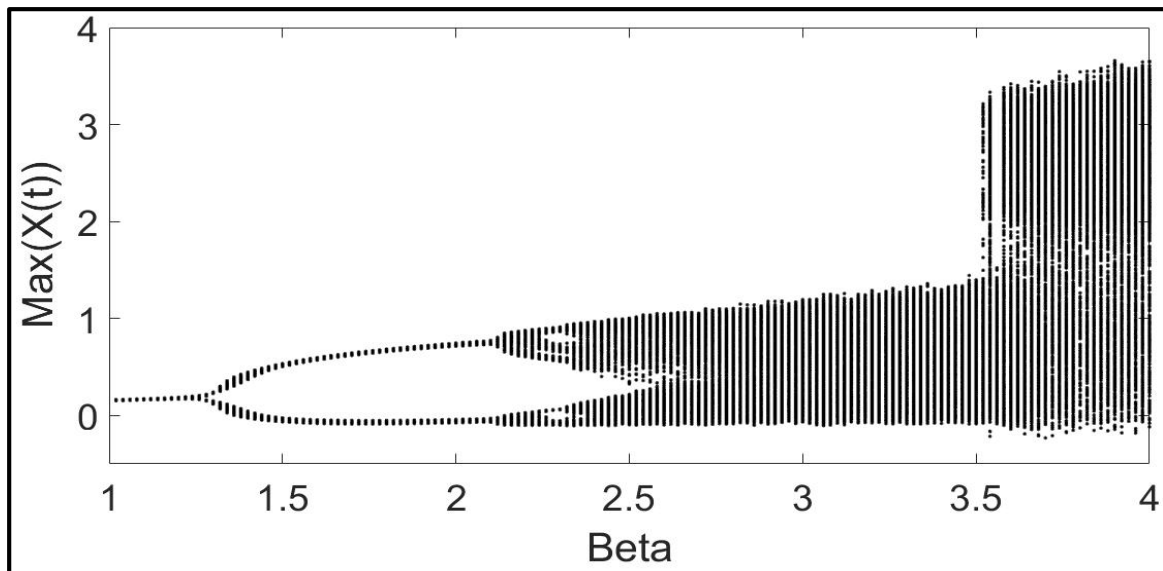


**Figure (9): Bifurcation diagram of maximum values of generated signals  $X(t)$  by OEO system as a function of nonlinear coefficient  $\beta$  control parameter.**

#### 4- Conclusion

Since the linear gain coefficient  $\beta$  is a function of different OEO system parameter, specially the laser optical power  $P_i$  and RF amplifier gain  $G$ ; hence it could be considered as control parameter for adjusting dynamical oscillation regimes. The numerical simulation of our OEO model in Eq. (3), showed miscellaneous transitions in dynamic oscillations, starting from period one, period doubling, mixed mode, quasi-periodic and chaotic oscillation, these transitions take place by increasing the value of  $\beta$ . These dynamical transitions were verified by the bifurcation diagram, which depicts the oscillation path of the OEO system into chaos.

## 5- References

- [1] Y.K. Chimbo "**Optoelectronic oscillators with time-delayed feedback**", REVIEWS OF MODERN PHYSICS, VOLUME 91, JULY–SEPTEMBER 2019
- [2] Y. K. Chembo, A. Hmima, P.A. Lacourt, L. Larger and J. M. Dudley, "**Generation of Ultralow Jitter Optical Pulses Using Optoelectronic Oscillators With Time-Lens Soliton-Assisted Compression**", JOURNAL OF LIGHTWAVE TECHNOLOGY, VOL. 27, NO. 22, NOVEMBER 15, 2009
- [3] Z. Zeng, L. Zhang, Y. WU, Z. Zhang, S. Zhang, B.Sun, and Y. Liu, "**Multi-format microwave signal generation based on an optoelectronic oscillator**", Optics Express 30834, Vol. 29, No. 19, 13 Sep 2021
- [4] J. Oden, R. Lavrov, Y. K. Chembo, and L. Larger, "**Multi-Gbit/s optical phase chaos communications using a time-delayed optoelectronic oscillator with a three-wave interferometer nonlinearity**", CHAOS 27, 114311 (2017)
- [5] Y.K. Chembo, "**Laser-based optoelectronic generation of narrowband microwave chaos for radars and radio-communication scrambling**", Optics Letters, Vol. 42, No. 17 / September 1 2017 .
- [6] L. Larger, A. B. Fuentes, R. Martinenghi, V. S. Udaltsov, Y. K. Chembo, and M. Jacquot, "**High-Speed Photonic Reservoir Computing Using a Time-Delay-Based Architecture: Million Words per Second Classification**", PHYSICAL REVIEW X 7, 011015 (2017)
- [7] Y.K. Chembo, "**Machine learning based on reservoir computing with time-delayed optoelectronic and photonic systems**", Chaos 30, 013111 (2020); doi: 10.1063/1.5120788
- [8] K. E. Callan, L. Illing, Z. Gao, D.J. Gauthier, and E. Scholl, "**Broadband Chaos Generated by an Optoelectronic Oscillator**", PHYSICAL REVIEW LETTERS, PRL 104, 113901 (2010) DOI:0.1103/PhysRevLett.104.113901
- [9] Y. C. Kouomou, P. Colet, L. Larger and N. Gastaud, "**Chaotic Breathers in Delayed Electro-Optical Systems**", PHYSICAL REVIEW LETTERS, PRL 95, 203903 (2005)
- [10] J.P. Goedgebuer, P. Levy, L. Larger, C. C. Chen, and W. T. Rhodes, "**Optical Communication with Synchronized Hyperchaos Generated Electro optically**", IEEE JOURNAL OF QUANTUM ELECTRONICS, VOL. 38, NO. 9, SEPTEMBER 2002
- [11] B. A. Marquez, L. Larger, D. Brunner, Y. K. Chemo, and M. Jacquot, "**Interaction between Lienard and Ikeda dynamics in a nonlinear electro-optical oscillator with delayed bandpass feedback**", PHYSICAL REVIEW E 94, 062208 (2016)
- [12] Kensuke IKEDA, "**Multiple-Valued Stationary state and its Instability of the Transmitted Light by a Ring-Cavity system**", OPTICS COMMUNICAT-IONS, Vol. 30, No. 2, August 1979
- [13] F. Marino, M. Ciszak, S.F. Abdalah, K. A. Al-Naimee, R. Meucci, F.T. Arecchi, "**Mixed-mode oscillations via canard explosions in light-emitting diodes with optoelectronic feedback**", Physical Review E, Vol.84, issue 4, 2011
- [14] Strogatz, S., H. (2018) *Nonlinear Dynamics and Chaos*. Second edition, by Taylor & Francis Group, LLC.P.2.